THE GERONTOLOGICAL SOCIETY OF AMERICA®

Journals of Gerontology: Biological Sciences
cite as: *J Gerontol A Biol Sci Med Sci*, 2021, Vol. 76, No. 5, 770–777
doi:10.1093/gerona/glaa248
Advance Access publication September 30, 2020

OXFORD

Original Article

Aging Influences the Metabolic and Inflammatory Phenotype in an Experimental Mouse Model of Acute Lung Injury

Kevin W. Gibbs, MD,[1,2] Chia-Chi Chuang Key, PhD,[3] Lanazha Belfield,[3] Jennifer Krall, MD,[1] Lina Purcell,[1] Chun Liu,[1] and D. Clark Files, MD[1,2,*]

[1]Department of Internal Medicine, Pulmonary, Critical Care, Allergy and Immunologic Diseases, Wake Forest School of Medicine, Winston-Salem, North Carolina. [2]Wake Forest Critical Illness, Injury, and Recovery Research Center, Wake Forest School of Medicine, Winston-Salem, North Carolina. [3]Department of Internal Medicine, Molecular Medicine, Wake Forest School of Medicine Winston-Salem, North Carolina.

*Address correspondence to: D. Clark Files, MD, Wake Forest School of Medicine, Medical Center Boulevard, Winston Salem, NC 27157. E-mail: clark.files@wakehealth.edu

Received: April 29, 2020; Editorial Decision Date: September 21, 2020

Decision Editor: Rozalyn M. Anderson, PhD, FGSA

Abstract

Increased age is a risk factor for poor outcomes from respiratory failure and acute respiratory distress syndrome (ARDS). In this study, we sought to define age-related differences in lung inflammation, muscle injury, and metabolism after intratracheal lipopolysaccharide (IT-LPS) acute lung injury (ALI) in adult (6 months) and aged (18–20 months) male C57BL/6 mice. We also investigated age-related changes in muscle fatty acid oxidation (FAO) and the consequences of systemic FAO inhibition with the drug etomoxir. Aged mice had a distinct lung injury course characterized by prolonged alveolar neutrophilia and lack of response to therapeutic exercise. To assess the metabolic consequences of ALI, aged and adult mice underwent whole body metabolic phenotyping before and after IT-LPS. Aged mice had prolonged anorexia and decreased respiratory exchange ratio, indicating increased reliance on FAO. Etomoxir increased mortality in aged but not adult ALI mice, confirming the importance of FAO on survival from acute severe stress and suggesting that adult mice have increased resilience to FAO inhibition. Skeletal muscles from aged ALI mice had increased transcription of key fatty acid metabolizing enzymes, CPT-1b, LCAD, MCAD, FATP1 and UCP3. Additionally, aged mice had increased protein levels of CPT-1b at baseline and after lung injury. Surprisingly, CPT-1b in isolated skeletal muscle mitochondria had decreased activity in aged mice compared to adults. The distinct phenotype of aged ALI mice has similar characteristics to the adverse age-related outcomes of ARDS. This model may be useful to examine and augment immunologic and metabolic abnormalities unique to the critically ill aged population.

Keywords: Critical illness, Fats, Inflammation, Nutrition

Acute respiratory distress syndrome (ARDS) is a devastating inflammatory lung disease characterized by bilateral pulmonary infiltrates, profound hypoxia, and respiratory failure (1). Direct pulmonary injury and indirect systemic insults such as sepsis can lead to ARDS. Consequently, this syndrome affects at least 200 000 individuals in the United States annually and is both a major cause of intensive care unit (ICU) admission and also a frequent complication of critical illness (2).

Older patients are particularly vulnerable to develop and die from ARDS. Patients older than 65 years of age have a 3-fold increase in ARDS incidence, increased mortality, prolonged mechanical ventilation, and increased organ failures compared to younger individuals (2–6). The importance of systemic complications in older individuals is further highlighted by long-term outcome data. Studies of ARDS survivors have demonstrated that older age is associated with longer lasting functional impairment after critical illness compared to younger cohorts (7–9).

Despite the clear clinical importance of aging in ARDS, older patients are frequently excluded from clinical trials, limiting our understanding of the clinical factors that mediate these differences

in outcomes (10). Animal models of lung injury are one method to further understand age-related disease mechanisms (11,12). Others have demonstrated in rodent models that aged animals develop more severe early alveolar inflammation and worsened oxidative lung injury (13–15). The intratracheal lipopolysaccharide (IT-LPS) model is a well-validated method of generating experimental acute lung injury in mice (16). IT-LPS results in robust and reproducible lung inflammation that allows for analysis of inflammatory mediators and promoters of injury resolution (17). Additionally, IT-LPS lung injury in mice induces muscle wasting which reproduces key features of muscle wasting in patients with ARDS and sepsis (18,19).

Our group has previously demonstrated that 2 days of exercise following IT-LPS in young-adult (8 weeks old) mice attenuates the lung injury and the skeletal muscle wasting phenotype (18). We have also shown that aged mice (18–20 months old) have increased mortality compared to adult mice (6 months old) and a skeletal muscle phenotype characterized by increased skeletal muscle lipid droplet accumulation and decreased muscle long-chain acylcarnitine after lung injury (20). Others have shown that skeletal muscle from critically ill patients exhibits mitochondrial dysfunction and impaired lipid oxidation (21–23). Collectively, these previously published data suggest that altered muscle metabolism may underlie the muscle wasting phenotype in age-related critical illness. Based on this prior work, we hypothesize that age-related vulnerability to ALI is in part mediated by inadequate skeletal muscle FAO due to impaired carnitine palmitoyltransferase-1 (CPT-1) activity, given that CPT-1 is the rate-limiting step in long-chain mitochondrial FAO. Additional objectives of our current study are to further define the age-related differences in lung and muscle injury in lung-injured mice with a focus on systemic and muscle fatty acid metabolism.

Methods

Animals and Acute Lung Injury Model

The Wake Forest School of Medicine Institutional Animal Care and Use Committee approved all procedures. Six-month (adult) and 18- to 20-month (aged) old male wild-type C57BL/6 mice (The National Institute of Health Aging Mouse Colony) were anesthetized with an intraperitoneal (i.p.) injection of 150 mg/kg ketamine and 13.5 mg/kg acetylpromazine and the trachea exposed. *Escherichia coli* lipopolysaccharide (O55:B5 L2880, lot 111M4035V, Sigma-Aldrich) (ALI mice) at 0.75 µg/g or an equivalent volume of sterile water (Sham mice) was instilled intratracheally using a 20-gauge catheter as previously described (19).

Bronchoalveolar Lavage Fluid Analysis

Bronchoalveolar lavage (BAL) was performed after euthanasia by exposing and cannulating the trachea with a 20-gauge catheter. The left lung was lavaged with sterile saline for a total volume return of approximately 1 mL. The recovered fluid was then centrifuged at 700*g* for 10 minutes. The cell-free supernatant was collected and stored at −80 °C. The cell pellet was resuspended in saline and stained with trypan blue. Total BAL cell count was calculated using a hemocytometer. BAL cell differential was determined using cytocentrifuge preparations (Cytospin 3; Shandon Scientific). Protein content in the cell-free supernatant was quantified using the Lowry colorimetric method (24).

Therapeutic Exercise

Mice were exercised in accordance with our previously published method. Exercise was performed on a 6-lane mouse treadmill (Columbus Instruments) at 0° incline using a graded protocol for 25 minutes duration twice daily. Speed was increased every 5 minutes from a starting speed of 5 m/min to a maximal speed of 9 m/min. Exercise regimens began 24 hours after IT-LPS instillation (day 1) and continued through day 2. Animals were sacrificed on day 3, 12 hours after the final treadmill exercise (18).

Cytokine ELISA

Plasma granulocyte colony-stimulating factor (G-CSF) was quantified using a mouse Quantikine ELISA kit (R&D systems) in accordance with manufacturer instructions (18). *TNF-α:* Plasma and BAL supernatant were isolated from adult and aged ALI and sham mice on day 3 or 4 after lung injury. To determine TNF-α protein levels, a mouse TNF-α Quantikine ELISA kit (R&D systems) was used per manufacturer instructions (25).

Metabolic Phenotyping

Indirect calorimetry was performed using a 6-chamber open circuit Oxymax/CLAMS unit (Columbus Instruments). Mice were individually housed and acclimatized for 12 hours in metabolic cages before hourly metabolic parameter recording began. Baseline measurements of respiratory exchange ratio (RER: the ratio of VCO_2/VO_2), energy expenditure (kcal/h), oxygen consumption (VO_2), carbon dioxide production (VCO_2), activity including x and z movement, and food consumption (g) were recorded hourly for 56 hours (26). The mice were then removed from the metabolic cages and returned to standard rodent housing for 72 hours. IT-LPS instillation was subsequently performed as described above. After recovery from anesthesia, the mice were returned to the metabolic cages and acclimatized for 12 hours. Hourly measurements of metabolic parameters were recorded for 148 hours before the mice were removed from the metabolic cages and sacrificed. Data from 1 aged animal were excluded after hour 84 post-LPS due to moribund status and impending death. Data from 1 adult animal were excluded after hour 121 due to development of peritonitis.

CPT-1 Inhibition

The non-specific CPT-1 inhibitor, etomoxir (Sigma-Aldrich), was dissolved in sterile water. About 15 µg/g body weight in 100 µL total volume was administered to aged and adult ALI and control mice on day 0 relative to IT-LPS (27).

Thiobarbituric Acid Reactive Substance Assay

Skeletal muscle lipid peroxidation was measured using a commercial kit (Cayman Chemical) to assay malondialdehyde formation in accordance with manufacturer instructions (28). Results were normalized for muscle protein content.

Isolation of Mitochondria From Skeletal Muscle

Mitochondria were isolated from gastrocnemius using previously described techniques (20). All centrifugation was carried out at 4 °C. Briefly, the gastrocnemius was dissected and non-muscle tissue was removed and placed in 500 µL of medium I (100 mM KCL, 5 mM $MGS0_4$*$7H_20$, 5 mM EDTA, 50 mM Tris–HCl, pH 7.4). The fresh muscle was blotted and weighed then placed in 1 mL of medium II (medium I and 1mM ATP, pH 7.4). The muscle was subsequently

minced with scissors and homogenized using a polytron homogenizer (3 × 15 seconds). An additional 500 µL of medium II was added to homogenate then centrifuged for 12,000 rpm for 15 minutes, to extract the subsarcolemmal mitochondrial fraction (supernatant). The subsarcolemmal mitochondrial fraction was collected and put on ice. The pellet was resuspended in 5 mL of medium II + protease inhibitor (Sigma P5380, 0.025 mL/g) for 5 minutes to isolate the intramyofibrillar mitochondria by further tissue digestion. An additional 15 mL of medium II was added and spun at 4200*g* for 10 minutes. The pellet was resuspended in 1 mL of medium II and spun at 12,000 rpm for 15 minutes to extract the intramyofibrillar mitochondria fraction (supernatant). Subsarcolemmal and intramyofibrillar mitochondrial fractions were combined and spun at 14,800 rpm for 15 minutes. The pellet (mitochondrial fraction) was washed with 1 mL of medium II and spun at 14,800 rpm for 15 minutes. The pellet was resuspended in 1 µL of medium III (220 mM sucrose, 70 mM mannitol, 10 mM Tris–HCl, and 1 mM EDTA, pH 7.4) per milligram of gastrocnemius muscle.

CPT-1 Activity

The protein concentration of isolated muscle mitochondria was determined by Pierce BCA Protein Assay and adjusted to be equal between samples (29). The reaction medium was prepared immediately as 117 mM Tris–HCl (pH 7.4), 0.28 mM reduced glutathione, 4.4 mM ATP, 4.4 mM $MgCl_2$, 16.7 mM KCL, 2.2 mM KCN, 40 mg/L rotenone, 0.5% BSA, 300 µM palmitoyl-CoA, and 5 mM L-carnitine and kept in a 37 °C water bath. Isolated mitochondria (10 µL) were then added in the reaction medium (90 µL) containing 1 µCi of L-[Methyl-^{3}H] carnitine hydrochloride (PerkinElmer NET1181250UC) in the absence or presence of malonyl-CoA (1 µL) in concentrations of 2, 5, and 10 µM. The reaction was stopped after 6 minutes by adding ice-cold 1 N HCl (0.5 ml). Palmitoyl-[^{3}H] carnitine was then extracted by adding water-saturated *n*-butanol (1 mL) and centrifuging at 1000*g* for 10 minutes. The top butanol layer containing palmitoyl-[^{3}H] carnitine was then removed and washed by adding *n*-butanol saturated water (2 mL). After centrifugation at 1000*g* for 10 minutes, the top butanol layer containing palmitoyl-[^{3}H] carnitine was transferred into a scintillation vial for radioactivity counting. CPT-1 activity was normalized to mitochondrial CPT-1 levels determined by western blot.

CPT-1 Western Blot

Muscle was homogenized using previously described techniques (13). Muscle mitochondria were isolated using the technique described above (29). The muscle-specific isotype CPT-1b was detected using a CPT-1b antibody (Proteintech, catalog number 22170-1-AP). Porin (Abcam, catalog number ab14734) was used as the housekeeping protein. Western blot densitometry was carried out using Image J software.

Real-Time qPCR

Muscle RNA was isolated using the trizol reagent, transcribed into cDNA and amplified with the appropriate primers using a one-step kit (Lo-Rox Bio 78005 Bioline) and a thermo cycler (7500 Fast real-time PCR system, Applied Biosystems). mRNA was normalized to GAPDH and mean fold change was calculated using the double delta CT method. All conditions were normalized relative to adult shams. TaqMan probe-based primers were used in all reactions for the following genes: CPT-1b (Thermofisher, catalog number 4331182), GAPDH (Applied Biosciences, catalog number 4352339E), mitochondrial uncoupling protein 3 (UCP3) (Thermofisher, catalog number 4331182), solute carrier family 27 member 1 (FATP1) (Thermofisher, catalog number Mm00449511_m1), medium chain acyl-coenzyme A dehydrogenase (MCAD) (Thermofisher, catalog number Mm01323360_g1), long-chain acyl-coenzyme A dehydrogenase (LCAD) (Thermofisher, catalog number Mm00599660_m1), peroxisome proliferative activated receptor gamma coactivator 1 alpha (PGC-1a) (Thermofisher, catalog number Mm01208835_m1)

Analysis

Analysis of the indirect calorimetry data was performed using baseline metabolic parameters as covariates to adjust for any differences that might exist between aged and adult mice before IT-LPS. Following lung injury, a repeated measures analysis of variance (ANOVA) modeled each parameter over the hours followed, adjusting baseline levels of the outcome measure to assess for differences between the 2 study groups. This ANOVA models the correlation within and between mice and adjusts appropriately for both sources of variance. An auto-regressive correlation structure was used to model these data. Wilcoxon rank sum tests were used to determine differences between individual day and night cycle metabolic parameters.

To determine differences in inflammatory parameters and lung physiology, Wilcoxon rank sums were performed comparing the outcome variable between the 2 groups.

Differences in survival between etomoxir-treated ALI mice, etomoxir-treated control mice and ALI mice were performed using the "survival" R package and *p* values were calculated by the log-rank test.

Statistical analysis was performed using R software and Graphpad Prism software. Graphs were generated using the "ggplot2" R package and Graphpad Prism.

Results

IT-LPS instillation produced robust alveolar inflammation in both adult and aged mice compared to controls (Figure 1A). At peak inflammation (day 2), adult ALI mice had higher BAL cell counts; however, BAL differentials and BAL protein were similar between age groups. TNFα levels (Figure 1A–D) were similar between the age groups on day 3 (aged) and day 4 (adult). Aged and adult mice exhibited distinct lung injury phenotypes. Despite having fewer alveolar cells on day 2, older mice had a higher percentage of BAL neutrophils on day 5 compared to adult mice, indicating prolonged acute lung injury and impaired injury resolution (Figure 1C, $p = .014$). Exercise further unmasked differences in this phenotype. Our group has previously demonstrated that therapeutic exercise in young-adult (8 weeks old) mice attenuated alveolar neutrophilia via reduction in systemic G-CSF and decreased IL-17 (18). The current study recapitulated this response in adult mice: exercise reduced the alveolar cell count in the adult age group (Figure 1E, $p = .006$). Unlike both young-adult and adult mice, aged ALI + exercise mice had no change in alveolar cell count after exercise, despite completion of the exercise protocol similarly to younger counterparts. Aged ALI mice additionally exhibited increased plasma GSCF compared to exercised adult ALI mice and a trend towards increased G-CSF in the ALI condition (Figure 1F).

Aged and adult mice also possessed distinct metabolic and feeding phenotypes after lung injury. Figure 2 shows the hourly

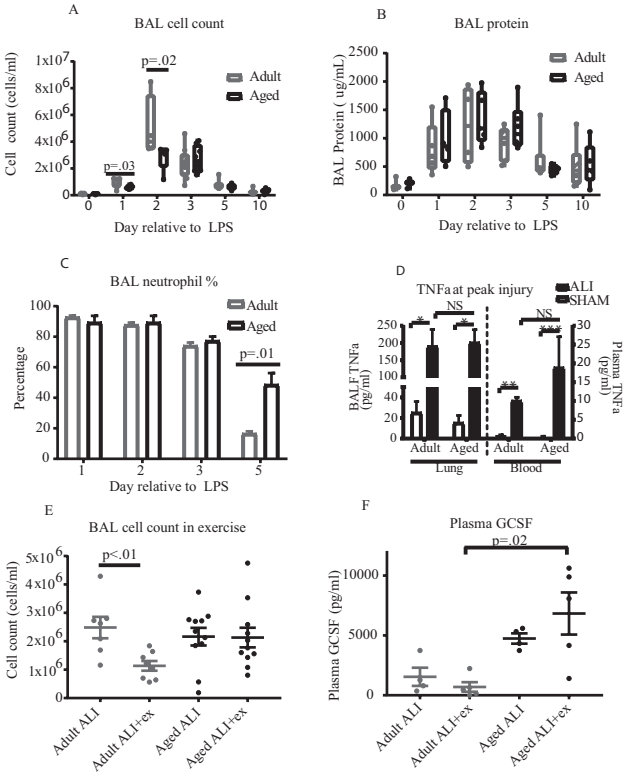

Figure 1. Comparison of injury and resolution patterns in aged and adult mice. (**A**) Aged and adult mice underwent alveolar lavage under sham and ALI conditions. Adult mice had a significantly higher BAL cell count at peak inflammation but similar counts at all other time points (group size 4–10 per time point). (**B**) BAL protein levels were measured in aged and adult mice. Protein levels were similar at all time points (group size 3–6 per time point). (**C**) Aged mice had prolonged alveolar neutrophilia compared to adult mice. BAL neutrophil percentage was similar at peak inflammation but increased in aged mice at day 5 (group size 4–10 per time point). (**D**) IT-LPS results in robust systemic and alveolar TNFα production. Aged and adult mice have similar TNFα levels in both BAL and blood after lung injury (group size 4–6). (**E**, **F**) Aged mice exhibit resistance to exercise. Exercise reduces alveolar cell count (group size 8–11) and plasma G-CSF (group size 4–5) in adult but not aged mice after lung injury.

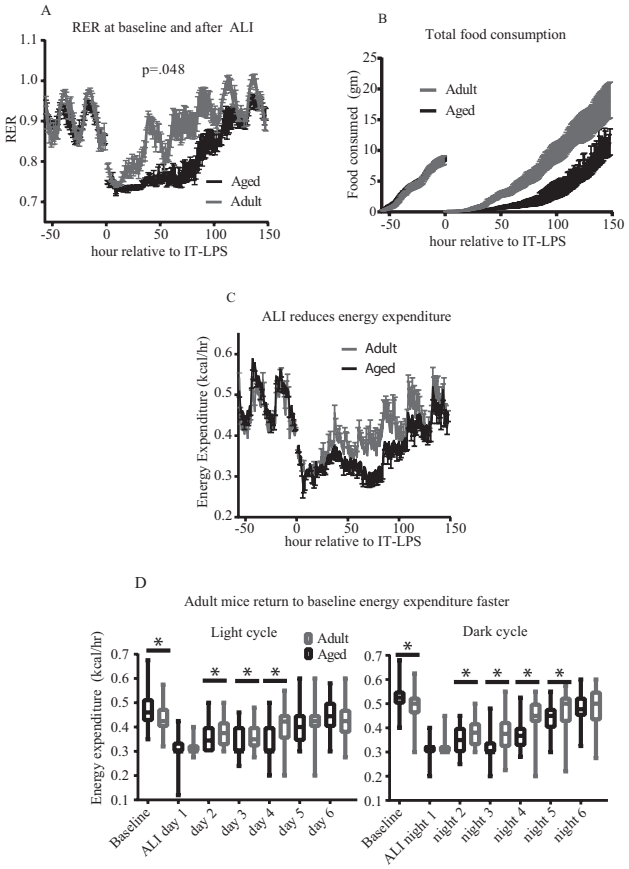

Figure 2. Aged and adult mice have distinct metabolic phenotypes after ALI. (**A**) Aged and adult mice were metabolically phenotyped before and after lung injury (n = 6 per group). Aged mice had significantly reduced (p = .048) RER after ALI compared to younger animals. (**B**) Aged and adult mice had similar food intake prior injury. Aged mice had prolonged anorexia and consumed significantly less food per hour after lung injury (p = .0003). (**C**, **D**). Both groups had decreased energy expenditure after ALI. When adjusting for baseline variation, differences in energy expenditure did not achieve statistical significance over the entire course of lung injury (p = .051). However, significant differences existed over individual light/dark cycles. Aged mice had higher energy expenditure at baseline, and reduced energy expenditure on light cycles 2–4 and dark cycles 2–5.

mean RER, food intake (g), and whole-subject energy expenditure (kcal/h). After adjusting for baseline variation between age groups, older animals had a significantly decreased RER after lung injury (Figure 2A, p = .048), indicating increased reliance on fatty acid metabolism. Older mice additionally had reduced hourly food intake (Figure 2B, p = .0003) and had significantly lower total food consumption on days 2–4 and strong trends on day 5 and 6 (Supplementary Figure 2A). Our statistical model also showed a near significant reduction in energy expenditure in aged animals (Figure 2C, p = .051). The metabolic chamber data showed substantial periodicity in metabolic parameters during each day/night cycle. We therefore analyzed individual dark/light cycles for age-related differences. Comparison between the age groups revealed that adult mice had a significantly higher RER at each 12-hour period with the exception of the preinjury light cycle during which aged mice had a higher RER (Supplementary Figure 1A, p < .05 baseline light cycle, p < .001 all other cycles). Intragroup comparison showed distinct patterns of substrate utilization after injury: adult mice had an RER elevated above baseline for each 12-hour period after day 3. In contrast, aged mice had a substantially reduced RER through night 5. Adult mice had a higher oxygen consumption (VO_2) during each time point. Intragroup analysis showed that whereas adult mice oxygen consumption returned to preinjury baseline by night 5, aged mice had a persistently reduced oxygen consumption throughout the duration of the metabolic experiment (Supplementary Figure 1C and D). A similar pattern was seen in carbon dioxide production (VCO_2). Adult mice had higher carbon dioxide production at all time points and returned to their baseline sooner than aged individuals (Supplementary Figure 1E and F). Older mice had higher whole-subject energy expenditure at baseline but decreased energy expenditure from light cycle 2–4 and night cycle 2–5. Adult mice returned to baseline sooner. Adult mice had increased x-axis movement at baseline and increased x- and z-axis movement after lung injury (Supplementary Figure 2E).

Skeletal muscle metabolism is a major determinant of total body energy expenditure and RER (30). We therefore

hypothesized that the age-specific metabolic phenotypes we observed were due to differences in skeletal muscle energy utilization. Our group has previously demonstrated that aged mice have both increased intramuscular lipid droplet accumulation and decreased long-chain acylcarnitines after ALI, suggesting aberrant fatty acid oxidation (FAO) (20). Others have shown that intraperitoneal injection of LPS reduces transcription of FAO enzymatic mediators in young-adult mouse diaphragm muscle (31). Based on these findings, we examined the effects of ALI on transcription of key enzymes involved in skeletal muscle FAO, UCP3(Figure 3A), CPT-1b (Figure 3B), LCAD (Figure 3C), FATP1 (Figure 3D), and MCAD (Figure 3E). Aged mice had significantly increased mean fold change in UCP3 at baseline and day 1 and 2 with trends towards increased levels on day 3 and 5 compared to adult mice (Figure 3A). To determine if the UCP3 changes were due to free radical generation, we examined skeletal muscle lipid peroxidation on day 1, 3, and 10. No difference was present between the 2 age groups at any time point, indicating UCP3 transcription due to FAO and not free radical generation. Aged mice have increased CPT-1b, FATP1, LCAD, and MCAD transcription at early time points compared to adults (Figure 3B–E). These data reveal that FAO genes undergo dynamic increases in transcription in skeletal muscle following ALI. ANOVA analysis showed significant differences between age and CPT-1b, UCP3, FATP1, LCAD, and MCAD fold change after injury. Because CPT-1 is the rate-limiting enzyme in fatty acid metabolism, we measured CPT-1b protein levels in isolated mitochondrial fractional lysates and performed CPT-1b activity assays at day 0 (baseline) and day 10 in adult and aged mice. Aged mice had increased CPT-1b protein levels compared to

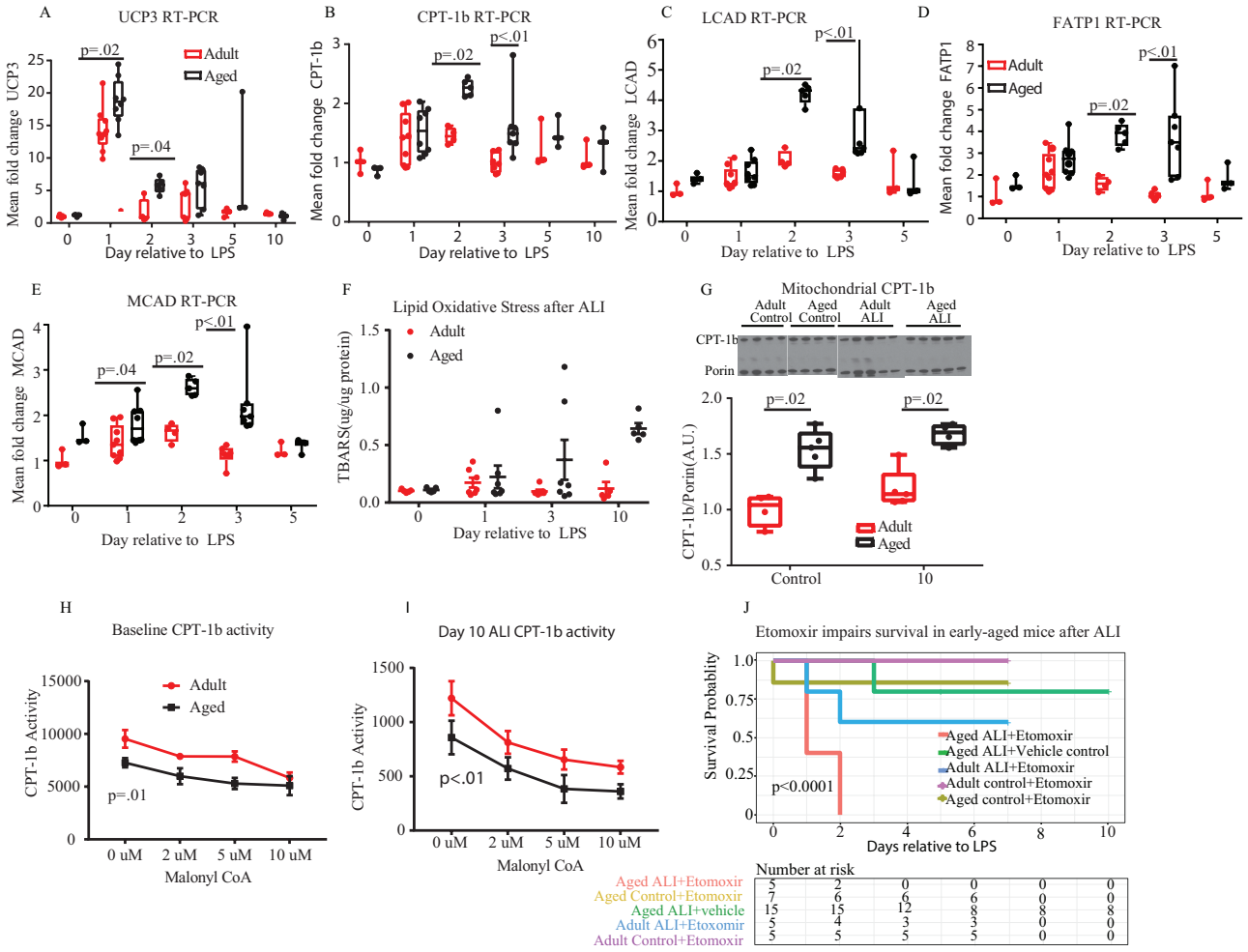

Figure 3. Comparison of fatty acid oxidation after ALI. (**A–E**) Transcription of key mediators of fatty acid oxidation (UCP3, CPT-1b, FATP1, MCAD, LCAD) was measured in gastrocnemius in aged and adult animals at baseline and after lung injury (group size 3–14 per time point). Transcription varied dynamically with IT-LPS. Aged mice consistently had higher transcription in early phase (day 1, 2, 3) ALI. (**F**) Oxidative stress was measured in skeletal muscle at baseline and after ALI by thiobarbituric acid reactive substance (TBARS) assay. No difference was seen at any time point (group size 5–7 per time point). (**G**) Mitochondrial CPT-1b protein expression was measured by western blot at baseline and day 10. Aged mice had increased CPT-1b expression at both baseline and day 10. Western blot was performed using 2 gels for electrophoresis. Same age baseline and day 10 injury were run on the same gel. (**H**) and (**I**) CPT-1b activity and malonyl inhibition were measured by radioassay at baseline and day 10 time points. Both aged and adult mice had increased CPT-1b activity at day 10 compared to baseline. Older mice had reduced activity when normalized for CPT-1 protein expression compared to younger animals. (**J**) Aged and adult mice were treated with either the CPT-1 inhibitor etomoxir or vehicle under control and ALI conditions. CPT-1 inhibition and ALI increased mortality in aged animals compared to vehicle or etomoxir alone. Aged ALI + vehicle control mice were sacrificed on day 10. All other conditions were sacrificed on day 7. All animals that survived to sacrifice showed signs of lung injury recovery.

adult mice at both time points (Figure 3G), though we found no change in CPT-1b protein levels following lung injury. CPT-1b activity was carried out using radiolabeled carnitine. We found that aged mice had decreased CPT-1b activity (normalized to CPT-1b protein level) at both baseline (Figure 3H) and 10 days (Figure 3I) after lung injury. The sensitivity of CPT-1b to inhibition by malonyl-CoA was not altered by age or LPS treatment.

To better determine whether mice were dependent on fatty acid metabolism after lung injury, we treated aged and adult mice with the FAO inhibitor, etomoxir. Etomoxir-treated aged ALI mice had increased mortality compared to vehicle-treated aged ALI mice and etomoxir-treated controls (Figure 3J). Mortality did not reach statistical significance in adult mice.

Discussion

In this study, we uncovered differential age-related immune and metabolic responses to lung injury using a mouse model of lung injury-induced muscle wasting. We found that aged mice with experimental lung injury exhibit an extended acute critical illness characterized by persistent alveolar neutrophilia, prolonged anorexia, increased dependence on fatty acid substrates but less effective FAO, and a failure to respond to exercise following lung injury. These differences, some of which are present at baseline (eg, CPT-1b muscle activity) and others which are brought out following lung injury/stress (eg, altered systemic metabolism), are potentially central to the differential age-related responses to lung injury and muscle weakness observed in older, critically ill humans.

Our group has previously demonstrated that older mice have both increased sensitivity to IT-LPS at higher doses and prolonged skeletal muscle weakness compared to adult mice (20). The current study establishes that at a reduced dose of 0.75 µg/g body weight, IT-LPS results in decreased alveolar cellularity at peak injury but prolonged alveolar neutrophilia in the older animals (Figure 1A and C). In human studies, persistent alveolar neutrophilia is associated with impaired lung injury resolution and increased ARDS mortality (32). Other researchers have identified increased alveolar neutrophilia in older animals after lung injury at very early time points (13–15). Our findings likely reflect model differences (direct lung injury with a reduced LPS dose) and distinct time points. Additionally, whereas adult mice have enhanced injury resolution with therapeutic exercise, we show that aged mice have persistent inflammation resistant to exercise therapy in the setting of elevated G-CSF (18). This systemic response is coupled with a failure of the exercise response to attenuate lung injury-induced muscle atrophy, seen in young and adult mice.

Consistent with impaired injury resolution, older mice have a distinct metabolic phenotype after ALI. Catabolism, anorexia, and lipolysis are conserved "acute phase" responses across mammalian species to critical illness (33,34). Whether these changes are adaptive or maladaptive remain unclear. In our study, older mice had a significantly prolonged decrease in RER (Figure 2A) and reduced food intake (Figure 2B) after lung injury, indicating an increased dependence on lipolysis and FAO for energy generation (35). These changes suggest protracted catabolism and impaired resolution of metabolic critical illness in the older animals. In contrast, the adult animals have early restoration of oxygen consumption, carbon dioxide production, energy expenditure, food intake, and a RER above baseline which reflect a recovered metabolic phenotype (36). We hypothesized that age-related vulnerability to ALI is in part mediated by impaired FAO in older individuals. This study demonstrates that aged animals have increased transcription of FAO mediators and prolonged dependence on FAO after lung injury. Despite the increased reliance on FAO, skeletal muscle from older animals had a significant decrease in the fatty acid metabolite long-chain acylcarnitines, suggesting that fatty acid metabolism may be uniquely impaired in skeletal muscle in older individuals with ARDS (20). The current study shows that despite elevated gene transcription of the rate-limiting enzyme in FAO, CPT-1b and increased CPT-1b protein expression, aged mice have decreased CPT-1 activity at both baseline and after lung injury. Decreased skeletal muscle CPT-1 protein levels has also been found in humans with critical illness (21). Thus, critical illness may unmask age-dependent impairment in FAO: Our study shows elevated transcription of key mediators of FAO (Figure 3A–E) without increased lipid peroxidation (Figure 3F) in aged animals suggesting that intramuscular lipid content may exceed mitochondrial capacity for FAO (37). Interestingly, our finding of increased transcription of FAO mediators in skeletal muscle from aged mice contrasts with previously published data of decreased transcription in diaphragm muscle after acute inflammation in younger animals (31). Age-related changes in fatty acid metabolism are intriguing potential pathophysiologic mechanisms in advanced-aged vulnerability to ARDS and its associated skeletal muscle dysfunction. Intramuscular lipid accumulation and mitochondrial fatty acid overload ("lipotoxicity") has been implicated as a cause of weakness and mitochondrial dysfunction in obesity (38). Effective fatty acid metabolism may be essential to preventing muscle dysfunction in critical illness as a recent study in a mouse model of sepsis demonstrated an association between preserved muscle strength and efficient fatty acid metabolism (39). Furthermore, acylcarnitines play an important role in resilience to acute stress. One recent study found that decreased acylcarnitine production worsened outcomes in older animals exposed to cold stress (40). The increased mortality with etomoxir treatment in our study (Figure 3J) supports the importance of effective FAO in the response to acute stress. Additionally, changes in skeletal muscle metabolism may account for ineffective exercise-mediated injury resolution seen in the older animals (20). Further investigation is needed to define this potential mechanism.

In conclusion, the current study demonstrates that the IT-LPS model successfully reproduces both adverse geriatric outcomes in ARDS and systemic complications. Importantly, these age-related differences highlight the heterogeneity of responses seen in patients with ARDS, some of which may be age-related. These differences are important to further understand, as older patients may need different treatments based on these differential immune mediated and metabolic responses during critical illnesses, such as ARDS and sepsis.

Supplementary Material

Supplementary data are available at *The Journals of Gerontology, Series A: Biological Sciences and Medical Sciences* online.

Funding

This work was supported by the Wake Forest Clinical and Translational Science Institute (CTSI) Ignition Fund (to K.G.); the Claude D. Pepper Older Americans Independence Center (P30AG21332); the National Institute of Diabetes and Digestive and Kidney Diseases at the National Institute of Health (DK117069 to C.-C.C.K.); and the National Institute of General Medical Sciences at the National Institute of Health (5K08GM123322-02 to D.C.F.).

Author Contributions

K.G. was responsible for experimental design, oversaw experiment conduct, performed analyses, and wrote the initial manuscript. C.-C.C.K. performed the metabolic phenotyping and CPT-1b activity assays, performed analyses, and assisted in manuscript preparation. L.B. contributed to mitochondrial isolation and manuscript preparation. J.K. assisted in data analysis and manuscript preparation. L.P. conducted key experiments and assisted in manuscript preparation. C.L. conducted key experiments and assisted in manuscript preparation. D.C.F. provided senior mentorship, oversaw experimental design, experiment conduct, and data analysis, and contributed substantially to manuscript preparation.

Conflicts of Interest

None declared.

References

1. Ranieri VM, Rubenfeld GD, Thompson BT, et al.; ARDS Definition Task Force. Acute respiratory distress syndrome: the Berlin Definition. *J Am Med Assoc*. 2012;307(23):2526–2533. doi:10.1001/jama.2012.5669
2. Rubenfeld GD, Caldwell E, Peabody E, et al. Incidence and outcomes of acute lung injury. *N Engl J Med*. 2005;353(16):1685–1693. doi:10.1056/NEJMoa050333
3. Suchyta MR, Clemmer TP, Elliott CG, et al. Increased mortality of older patients with acute respiratory distress syndrome. *Chest*. 1997;111(5):1334–1339. doi:10.1378/chest.111.5.1334
4. Milberg JA, Davis DR, Steinberg KP, Hudson LD. Improved survival of patients with acute respiratory distress syndrome (ARDS): 1983–1993. *J Am Med Assoc*. 1995;273(4):306–309. doi:10.1001/jama.1995.03520280052039
5. Ely EW, Wheeler AP, Thompson BT, Ancukiewicz M, Steinberg KP, Bernard GR. Recovery rate and prognosis in older persons who develop acute lung injury and the acute respiratory distress syndrome. *Ann Intern Med*. 2002;136(1):25–36.
6. Amato MB, Meade MO, Slutsky AS, et al. Driving pressure and survival in the acute respiratory distress syndrome. *N Engl J Med*. 2015;372(8):747–755. doi:10.1056/NEJMsa1410639
7. Herridge MS, Chu LM, Matte A, et al.; RECOVER Program Investigators (Phase 1: towards RECOVER); Canadian Critical Care Trials Group. The RECOVER program: disability risk groups and 1-year outcome after 7 or more days of mechanical ventilation. *Am J Respir Crit Care Med*. 2016;194(7):831–844. doi:10.1164/rccm.201512-2343OC
8. Herridge MS, Tansey CM, Matté A, et al.; Canadian Critical Care Trials Group. Functional disability 5 years after acute respiratory distress syndrome. *N Engl J Med*. 2011;364(14):1293–1304. doi:10.1056/NEJMoa1011802
9. Ehlenbach WJ, Larson EB, Curtis JR, Hough CL. Physical function and disability after acute care and critical illness hospitalizations in a prospective cohort of older adults. *J Am Geriatr Soc*. 2015;63(10):2061–2069. doi:10.1111/jgs.13663
10. Cooke CR, Erickson SE, Watkins TR, Matthay MA, Hudson LD, Rubenfeld GD. Age-, sex-, and race-based differences among patients enrolled versus not enrolled in acute lung injury clinical trials. *Crit Care Med*. 2010;38(6):1450–1457. doi:10.1097/CCM.0b013e3181de451b
11. Huizer-Pajkos A, Kane AE, Howlett SE, et al. Adverse geriatric outcomes secondary to polypharmacy in a mouse model: the influence of aging. *J Gerontol A Biol Sci Med Sci*. 2016;71(5):571–577. doi:10.1093/gerona/glv046
12. Cordeiro AV, Brícola RS, Braga RR, et al. Aerobic exercise training induces the mitonuclear imbalance and UPRmt in the skeletal muscle of aged mice. *J Gerontol A Biol Sci Med Sci*. 2020 Mar 16. doi:10.1093/gerona/glaa059
13. Linge HM, Lee JY, Ochani K, et al. Age influences inflammatory responses, hemodynamics, and cardiac proteasome activation during acute lung injury. *Exp Lung Res*. 2015;41(4):216–227. doi:10.3109/01902148.2014.999174
14. Linge HM, Ochani K, Lin K, Lee JY, Miller EJ. Age-dependent alterations in the inflammatory response to pulmonary challenge. *Immunol Res*. 2015;63(1-3):209–215. doi:10.1007/s12026-015-8684-7
15. Starr ME, Ueda J, Yamamoto S, Evers BM, Saito H. The effects of aging on pulmonary oxidative damage, protein nitration, and extracellular superoxide dismutase down-regulation during systemic inflammation. *Free Radic Biol Med*. 2011;50(2):371–380. doi:10.1016/j.freeradbiomed.2010.11.013
16. Chen H, Bai C, Wang X. The value of the lipopolysaccharide-induced acute lung injury model in respiratory medicine. *Expert Rev Respir Med*. 2010;4(6):773–783. doi:10.1586/ers.10.71
17. D'Alessio FR, Tsushima K, Aggarwal NR, et al. $CD4^+CD25^+Foxp3^+$ Tregs resolve experimental lung injury in mice and are present in humans with acute lung injury. *J Clin Invest*. 2009;119(10):2898–2913. doi:10.1172/JCI36498
18. Files DC, Liu C, Pereyra A, et al. Therapeutic exercise attenuates neutrophilic lung injury and skeletal muscle wasting. *Sci Transl Med*. 2015;7(278):278ra32. doi:10.1126/scitranslmed.3010283
19. Files DC, D'Alessio FR, Johnston LF, et al. A critical role for muscle ring finger-1 in acute lung injury-associated skeletal muscle wasting. *Am J Respir Crit Care Med*. 2012;185(8):825–834. doi:10.1164/rccm.201106-1150OC
20. Files DC, Ilaiwy A, Parry TL, et al. Lung injury-induced skeletal muscle wasting in aged mice is linked to alterations in long chain fatty acid metabolism. *Metabolomics*. 2016;12(134):1079–1075. doi:10.1007/s11306-016-1079-5
21. Puthucheary ZA, Astin R, Mcphail MJW, et al. Metabolic phenotype of skeletal muscle in early critical illness. *Thorax*. 2018;73:926–935. doi:10.1136/thoraxjnl-2017-211073
22. Singer M. Critical illness and flat batteries. *Crit Care*. 2017;21(Suppl. 3):309. doi:10.1186/s13054-017-1913-9
23. Singer M. The role of mitochondrial dysfunction in sepsis-induced multi-organ failure. *Virulence*. 2014;5(1):66–72. doi:10.4161/viru.26907
24. Peterson GL. A simplification of the protein assay method of Lowry *et al*. which is more generally applicable. *Anal Biochem*. 1977;83(2):346–356. doi:10.1016/0003-2697(77)90043–4
25. Seemann S, Lupp A. Administration of a CXCL12 analog in endotoxemia is associated with anti-inflammatory, anti-oxidative and cytoprotective effects in vivo. *PLoS One*. 2015;10(9):e0138389. doi:10.1371/journal.pone.0138389
26. Kandasamy AD, Sung MM, Boisvenue JJ, Barr AJ, Dyck JR. Adiponectin gene therapy ameliorates high-fat, high-sucrose diet-induced metabolic perturbations in mice. *Nutr Diabetes*. 2012;2:e45. doi:10.1038/nutd.2012.18
27. Shriver LP, Manchester M. Inhibition of fatty acid metabolism ameliorates disease activity in an animal model of multiple sclerosis. *Sci Rep*. 2011;1:79. doi:10.1038/srep00079
28. Ono T, Takada S, Kinugawa S, Tsutsui H. Curcumin ameliorates skeletal muscle atrophy in type 1 diabetic mice by inhibiting protein ubiquitination. *Exp Physiol*. 2015;100(9):1052–1063. doi:10.1113/EP085049
29. Bruce CR, Brolin C, Turner N, et al. Overexpression of carnitine palmitoyltransferase I in skeletal muscle in vivo increases fatty acid oxidation and reduces triacylglycerol esterification. *Am J Physiol Endocrinol Metab*. 2007;292(4):E1231–E1237. doi:10.1152/ajpendo.00561.2006

30. Zurlo F, Larson K, Bogardus C, Ravussin E. Skeletal muscle metabolism is a major determinant of resting energy expenditure. *J Clin Invest*. 1990;86(5):1423–1427. doi:10.1172/JCI114857
31. Feingold KR, Moser A, Patzek SM, Shigenaga JK, Grunfeld C. Infection decreases fatty acid oxidation and nuclear hormone receptors in the diaphragm. *J Lipid Res*. 2009;50(10):2055–2063. doi:10.1194/jlr.M800655-JLR200
32. Steinberg KP, Milberg JA, Martin TR, Maunder RJ, Cockrill BA, Hudson LD. Evolution of bronchoalveolar cell populations in the adult respiratory distress syndrome. *Am J Respir Crit Care Med*. 1994;150(1):113–122. doi:10.1164/ajrccm.150.1.8025736
33. Van den Berghe G. On the neuroendocrinopathy of critical illness. Perspectives for feeding and novel treatments. *Am J Respir Crit Care Med*. 2016;194(11):1337–1348. doi:10.1164/rccm.201607-1516CI
34. Rittig N, Bach E, Thomsen HH, et al. Regulation of lipolysis and adipose tissue signaling during acute endotoxin-induced inflammation: a human randomized crossover trial. *PLoS One*. 2016;11(9):e0162167. doi:10.1371/journal.pone.0162167
35. Turner N, Bruce CR, Beale SM, et al. Excess lipid availability increases mitochondrial fatty acid oxidative capacity in muscle: evidence against a role for reduced fatty acid oxidation in lipid-induced insulin resistance in rodents. *Diabetes*. 2007;56(8):2085–2092. doi:10.2337/db07-0093
36. Chiolero R, Revelly JP, Tappy L. Energy metabolism in sepsis and injury. *Nutrition*. 1997;13(Suppl. 9):45S–51S. doi:10.1016/S0899-9007(97)00205-0
37. Schrauwen P, Hinderling V, Hesselink MK, et al. Etomoxir-induced increase in UCP3 supports a role of uncoupling protein 3 as a mitochondrial fatty acid anion exporter. *FASEB J*. 2002;16(12):1688–1690. doi:10.1096/fj.02-0275fje
38. Tumova J, Andel M, Trnka J. Excess of free fatty acids as a cause of metabolic dysfunction in skeletal muscle. *Physiol Res*. 2016;65(2):193–207. doi:10.33549/physiolres.932993
39. Goossens C, Marques MB, Derde S, et al. Premorbid obesity, but not nutrition, prevents critical illness-induced muscle wasting and weakness. *J Cachexia Sarcopenia Muscle*. 2017;8(1):89–101. doi:10.1002/jcsm.12131
40. Simcox J, Geoghegan G, Maschek JA, et al. Global analysis of plasma lipids identifies liver-derived acylcarnitines as a fuel source for brown fat thermogenesis. *Cell Metab*. 2017;26(3):509–522.e6. doi:10.1016/j.cmet.2017.08.006